frontiers | Frontiers in Energy Research

TYPE Original Research
PUBLISHED 06 July 2023
DOI 10.3389/fenrg.2023.1199442

OPEN ACCESS

EDITED BY
Tao Zhang,
University of Science and Technology Beijing, China

REVIEWED BY
Dehao Qin,
Clemson University, United States
Aleksandar Janjic,
University of Niš, Serbia, Serbia
Muhammad Aziz,
The University of Tokyo, Japan

*CORRESPONDENCE
Chen Peng,
chen.peng@jsu.edu.cn

RECEIVED 03 April 2023
ACCEPTED 09 June 2023
PUBLISHED 06 July 2023

CITATION
Peng C and Niu Y (2023), Optimal serving strategy for vehicle-to-grid business: service agreement, energy reserve estimation, and profit maximization. *Front. Energy Res.* 11:1199442. doi: 10.3389/fenrg.2023.1199442

Optimal serving strategy for vehicle-to-grid business: service agreement, energy reserve estimation, and profit maximization

Chen Peng[1]* and Yajie Niu[2]

[1]College of Information Science and Engineering, Jishou University, Jishou, China, [2]School of Communication and Electronic Engineering, Jishou University, Jishou, China

To advocate the adoption of electric vehicle (EV) technologies, this paper studies a practical operating paradigm for running a charge park vehicle-to-grid (V2G) service business. The operating paradigm consists of a service agreement and two consecutive day-ahead analyses. Specifically, i) the service agreement underpins the communication pattern between the EV owners and the V2G service operator, ii) day-ahead analysis-I estimates the V2G energy reserve distribution, and iii) day-ahead analysis-II aims to maximize profit by optimizing decision variables for the scheduled day, such as the output period and sale price of the V2G energy. Correspondingly, the contributions of this paper are three-fold. First, the major principles behind the design of a service agreement are highlighted, and a practical service agreement that abides by the principle is formed. Second, for day-ahead analysis-I, this paper proposes a V2G energy reserve modeling method for the rapid estimation of V2G energy reserve distribution, which is applied to a case study of New York City working and recreational environment charge parks. Third, for day-ahead analysis-II, an evaluation framework is proposed, which provides various metrics for characterizing the V2G output capacity. The metrics evaluation and profit maximization methods are presented with theoretical results and are verified also by computer experiments. For example, we show that for the simulated environment with peak time-of-use hours [13:00, 16:00] and V2G output period [13:00, 14:00], the V2G output power threshold 61 kW selected by our method achieves almost the maximum scheduled day profit (true maximum achieved at 60 kW).

KEYWORDS

vehicle-to-grid service, energy reserve distribution, service agreement, day-ahead analysis, profit optimization

1 Introduction

The present and continuously increasing penetration of electric vehicles (EVs) presents various challenges to the power system. Meanwhile, it has been widely recognized that EV batteries can provide various auxiliary services to the power system, by supplying excessive energy back to the grid. The foundation of such activities is the so-called

vehicle-to-grid (V2G) technology, which is enabled by novel bidirectional chargers (Suul et al., 2016; Szinai et al., 2020; Popkova et al., 2023).

According to the objectives and locations of charging, the currently envisioned EV charging services (along with the existing services) can be classified into the following three major scenarios: commercial charging (CC), business charging (BC), and home charging (HC) (Islam et al., 2018). Specifically, CC refers to dedicated fast charging services aimed to extend EV distances, which functions as a future gas station equivalent and uses DC fast charging stations (FCSs) with the highest charging level (level 3) (Yunus et al., 2011; Fan et al., 2015; Zhang et al., 2022). BC refers to charging services integrated with business premises (level 2) (Islam et al., 2018; Yan et al., 2018; Jin and Tan, 2019), such as shopping malls, universities, and offices, in order to provide welfare and attract EV owners, benefiting the whole integrated system. Finally, HC refers to charging that usually happens at home with an ordinary household outlet (level 1) and is also referred to as residential charging (Richardson et al., 2012; Maigha and Crow, 2017; Jin and Zhao, 2018).

Compared to CC and HC, BC charge parks are most likely to pioneer the collective use of V2G technology (Gough et al., 2017; Yan et al., 2018) since efficiency is most prioritized in CC (Bayram et al., 2012; Mauri and Valsecchi, 2012; Shan et al., 2019), and HC users already have a considerable time flexibility for satisfying charging demands, not to mention upgrading the existing infrastructures (Lopez-Behar et al., 2019; Zhao et al., 2020).

However, the adoption of V2G technology in charge parks is still facing several challenges. First, it has been investigated that in many circumstances, EV drivers prefer not to participate in V2G contracts—they are mostly concerned about the "discharging cycles" and the "guaranteed minimum battery level" (Hu et al., 2021; Huang et al., 2021). Second, the uncertainties from user behaviors are very difficult to model due to the lack of a generally recognized V2G serving agreement and the intrinsic randomness of user behaviors. As a result, researchers adopt different assumptions on the service agreements, and the results of different studies are hard to compare (Nguyen et al., 2016; Gough et al., 2017; Uddin et al., 2017; Lakshminarayanan et al., 2018).

In recent years, several studies in the field of V2G focus on efficient charging strategies and grid stability maintenance. For example, in the work of Qin et al. (2020), a bidirectional photovoltaic/battery-assisted EV parking lot system was proposed with V2G service, effectively managing EVs' charging and discharging states to support grid stability. However, a prerequisite for implementing these functionalities lies in accurately predicting the user demands and, consequently, being able to further forecast the capacity of V2G services provided by charge parks. Currently, there is limited research that explicitly addresses the challenges associated with the predicting user demands. Therefore, one of the novelties of this paper is to propose a service agreement aimed at mitigating the uncertainty of user behavior.

To facilitate the adoption of EV technologies, this paper considers a practical operating paradigm for running a charge park V2G service business. The operating paradigm consists of four steps, i.e., determining a service agreement, day-ahead analysis-I, day-ahead analysis-II, and executing the optimal decision. Specifically, i) the service agreement underpins the communication pattern between the EV owners and the V2G service operator. ii) Day-ahead analysis-I aims to identify the time with abundant V2G energy, based on the service agreement. iii) Day-ahead analysis-II is performed for profit maximization through specifying the V2G scheduler model and searching for the optimal decision variables. iv) Finally, the optimal decisions are executed on the scheduled day.

The major contributions of this paper are summarized as follows:

1. The V2G business operating paradigm is proposed, which consists of forming a service agreement, day-ahead analyses-I, day-ahead analyses-II, and decision execution. In addition, the major principles behind the design of a service agreement are highlighted, and a practical service agreement that abides by the principles is formed.
2. For day-ahead analysis-I, based on the service agreement, a V2G energy reserve estimation method is developed to identify the time with abundant V2G energy. The method is applied in a case study of New York City working and recreational environment charge parks, and the time with abundant V2G energy agrees with the results given by day-ahead analysis-II.
3. For day-ahead analysis-II, the mixed-integer linear programming (MILP) V2G scheduler model is considered, based on which an evaluation framework is proposed to characterize the V2G service output capability. Specifically, the evaluation framework provides metrics for characterizing the V2G output power capacity, service cost, and profit, as well as the methods to compute the metrics, which are verified theoretically and experimentally.

This paper is organized as follows. Section 2 introduces related studies. In Section 3, the V2G business operating paradigm is described and a practical V2G service agreement is formed. In Section 4, for day-ahead analysis-I, a V2G energy reserve modeling method is developed and applied to a case study of New York City working and recreational environment charge parks. Next, for day-ahead analysis-II, Section 5 considers a MILP V2G scheduler model, based on which several evaluation metrics are introduced to characterize the V2G service capability. In Section 6, the metrics evaluation and profit maximization methods are presented with theoretical results and are verified also by computer experiments. Finally, Section 7 concludes the paper.

2 Related studies

2.1 User behavior and service agreement

As pointed out in the work of Nguyen et al. (2016), customer requirements from EV owners are highly dependent on personal preferences. The common serving strategies in the literature can be classified into the following two categories: prediction-based serving and user-specification-based serving.

As examples of prediction-based serving, Gough et al. (2017), Uddin et al. (2017), and Wu et al. (2022) assumed that the energy of the next trip can be predicted accurately. Thus, EVs were discharged to the lowest possible level to exactly satisfy the next trip's energy requirement. The predictions were made by the V2G aggregator in the work of Gough et al. (2017) and Song et al. (2020) and by the battery management system (BMS) in the work of

Uddin et al. (2017) and Zhu et al. (2021), which were overambitious. Similarly, in the work of Lakshminarayanan et al. (2018), EV travel patterns were forecasted using a random-forest forecasting method. The predictions provided information on the EVs' future trips at specified intervals and the EVs' dwell time in that day.

In user-specification-based serving, EV owners provided departure times and the desired disconnection SoCs before starting the connection services (Nguyen et al., 2016; Yan et al., 2018; Li C. et al., 2020). The EV owners might also specify other preferences as inputs, such as the maximum V2G power and energy. Such a policy minimized the need for predictions; however, a higher level of user engagement is required.

In summary, the majority of current modeling approaches for V2G charge parks were either assuming overambitious predictive service agreements (Gough et al., 2017; Wang et al., 2015; Shi et al., 2023) or were constructed to be very complicated to account for various user preferences, assuming highly user-engaging serving patterns (Yan et al., 2018; Huo et al., 2016; Nguyen et al., 2016). The absence of a well-established V2G service agreement results in large discrepancies on how to model user behaviors.

2.2 Capacity prediction and V2G scheduling

Many studies in the field of V2G currently focus on efficient charging strategies and grid stability maintenance. For example, in the work of Qin et al. (2020), a bidirectional photovoltaic/battery-assisted EV parking lot system was proposed with V2G service, thus effectively managing EVs' charging and discharging states to support grid stability. However, a prerequisite for implementing these functionalities lies in accurately predicting user demands and, consequently, being able to further forecast the capacity of V2G services provided by charge parks. Due to the complexity of the user demand and EV travel patterns, the accurate prediction of the user demand is difficult. One appealing alternative problem is V2G capacity prediction, which predicts the potential of V2G service providers instead. As indicated in the work of Zhang et al. (2016), V2G capacity was highly dependent on charging/discharging schedules, according to the analysis of two extreme plans. Based on the work of Zhang et al. (2016), a V2G capacity evaluation method for the shift-working V2G was proposed in the work of Dai et al. (2020), where an analytical solution can be derived. In the work of Li S. et al. (2020), the V2G schedulable capacity was simulated and predicted with the dynamic rolling prediction and decision method.

Generally speaking, V2G schedulers are modeled so that the factors of charging stations, power grid, and user satisfaction are captured. Different optimization objectives can be pursued, which include minimizing carbon dioxide emissions (Hoehne and Chester, 2016; Ravi and Aziz, 2022) and maximizing profit (Huda et al., 2020; Chai et al., 2023) and user satisfaction (Triviño-Cabrera et al., 2019; Singh et al., 2023). For example, Ravi and Aziz (2022) mentioned that V2G technology, along with the diversification of clean fuels in the mobility sector, will help address the larger issue of climate change and carbon emissions more effectively than traditional methods. In the work of Huda et al. (2020), in JAMALI, Indonesia, the peak-hour supply was reduced by up to 2.8% (coal) and 8.8% (gas), with potential cost reductions of up to 60.15% and a 3.65% increase in power companies' annual revenue through V2G implementation. In the work of Singh et al. (2023), a novel power loss reduction index was introduced to ensure the delivery of high-quality power supply to users, and the effectiveness of the proposed indicator was validated through experiments. For the survival of a V2G business, maximizing profit while satisfying user demand and reducing charge anxiety is crucial (Varshosaz et al., 2019).

3 Operating paradigm and the service agreement

In this section, the V2G business operating paradigm is described. Then, the major principles behind the design of a service agreement are highlighted, and a practical service agreement that abides by the principle is formed in order to facilitate the modeling and analysis of V2G energy.

3.1 The V2G business operating paradigm

The V2G business operating paradigm involves the determination of a service agreement, day-ahead analysis-I, day-ahead analysis-II, and the execution of the optimal decision, as shown in Figure 1. Specifically,

1. The service agreement is a basis for the V2G business, which underpins the communication pattern between EV owners and the V2G service operator. Therefore, the service agreement must be determined before the scheduling model can be formulated, which is again a basis for any further analysis.
2. Day-ahead analysis-I is a fast version of day-ahead analysis, which aims to quickly estimate the V2G energy reserve distribution and identify the time with abundant V2G energy, based on the service agreement and historical data. It is expected to be fast since no scheduler model needs to be considered at this step.
3. Day-ahead analysis-II is a more complicated version of day-ahead analysis, which is performed for profit maximization through specifying the V2G scheduler model and searching for the optimal decision variables, such as the V2G output time interval, output power, and V2G energy sale price.
4. The final step is the execution of the optimal decisions on the scheduled day.

It can be seen that the service agreement should be determined before starting the V2G business, and the day-ahead analyses I and II constitute the main planning stage, which are to be conducted 1 day before the scheduled day, and these are our main research targets. The execution of decision variables is not covered in this paper.

3.2 Service agreement

A well-designed service agreement should satisfy the following requirements: i) the transaction rule is straightforward enough for the EV owners to comprehend and comply with; ii) the agreement should be based on a conventional parking policy, e.g., a flat fee for parking a certain number of hours or days, with additional

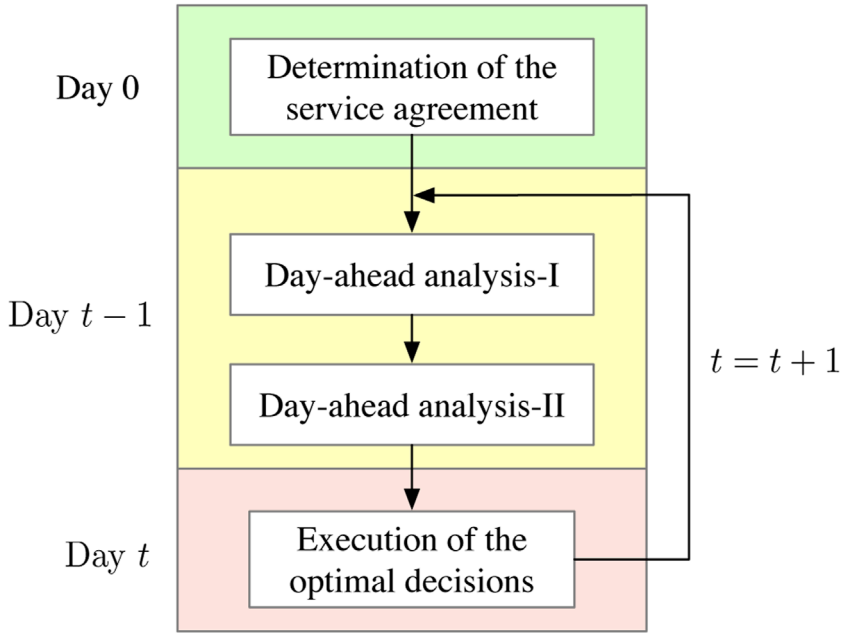

FIGURE 1
V2G business operating paradigm.

commitments to charging/discharging; and iii) the agreement is in accordance with the system operator's interests, which include reducing the EV charging costs and facilitating the usage of V2G technologies.

Therefore, assuming that the BC charge park uses level 2 chargers (6.6 kW) uniformly for all EV parking spaces, we consider the following charging agreement: "*after plugging in the charger, each EV owner chooses a predicted dwell time and then the system operator will be committed to charging the EV with an average power of* p_{ca} *by the end of the set dwell time or up to an SoC upper limit* $s^{max} < 1$, *while gaining the right to discharge the EV's battery during this period, as needed; the operator will not be responsible for failing to satisfy the commitment if the EV departs before reaching the set dwell time.*" It should be noted that the only action EV owners are required to do, besides plugging in, is to determine a dwell time. This service agreement is intended to be used in conjunction with a conventional parking policy (free parking or hourly flat fee for the parking lots); thus, it can be free of charge, or an additional hourly flat fee can be used for parking. The proposed service agreement satisfies the three requirements of the design.

4 Day-ahead analysis-I: estimating V2G energy reserve distribution

4.1 V2G energy reserve modeling

In this section, we omit the subscript v, referring to each EV for simplicity. Using the known arrival time t_0 and set dwell time T, the departure time of an EV can be derived as $t_f = t_0 + T$. Since the average charging power p_{ca} is given, the committed increased battery energy E^{target} and the departure SoC s^{target} are given by

$$E^{target} = \min\left\{p_{ca}T, B\left(s^{max} - s_0\right)\right\}, \tag{1}$$

$$s^{target} = S(t_f) = s_0 + E^{target}/B, \tag{2}$$

where B is the EV's battery capacity. It should be that s^{max} is usually a scalar close to but smaller than 1, such as 0.95, for protection and efficiency purposes Fan et al. (2015).

4.1.1 Modeling the extreme cases

Every EV's charging process has two extreme cases, i.e., first charge with the maximum charging power and then discharge with the maximum discharging power or first discharge with the maximum discharging power and then charge with the maximum charging power. The extreme cases seldom appear and usually should be avoided. However, it is useful to consider one extreme case for modeling the EV-based energy storage.

Here, we use the second case (maximum discharge before charging) to derive the design of an EV's initial V2G energy $r(t_0)$ and then consider general cases to design the V2G energy function $r(t)$. With the committed increased battery energy E^{target} and departure SoC s^{target} computed with Eqs 1, 2, and assuming that the initial SoC s_0 is high enough to prevent discharging at the lower limit of SoC, the charging process of an EV is shown in Figure 2A.

Here, t_1 is the latest time to stop discharging and start charging with full charging power, and t_2 is the latest time to start charging if no discharge activities happen. The time instants t_1 and t_2 are given by

$$t_1 = \frac{p_d t_0 + p_c t_f - E^{target}}{p_d + p_c}, \tag{3}$$

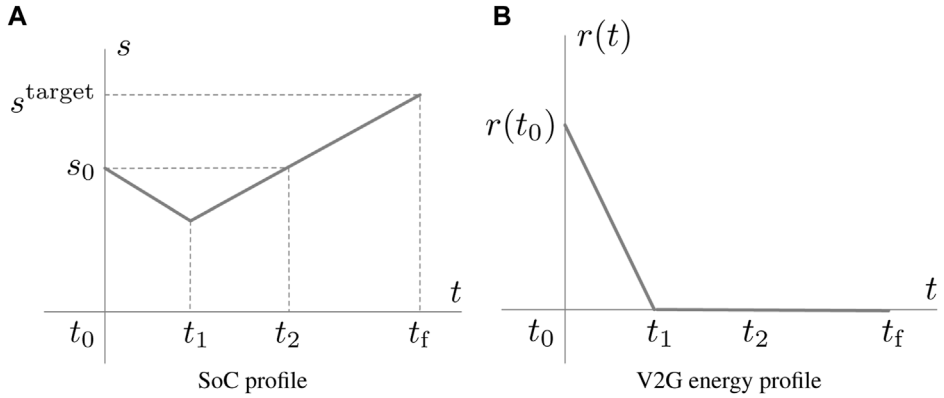

FIGURE 2
SoC and V2G energy reserve profiles in the second extreme case (maximally discharge before charging).

$$t_2 = t_f - E^{\text{target}}/p_c, \tag{4}$$

where p_d and p_c denote the maximum discharging and charging powers, respectively.

Then, the V2G energy reserve $r(t)$ in this case can be derived as follows. Since V2G energy reserve refers to the amount of energy stored in a battery that can be discharged for V2G purposes, the profile of $r(t)$ should be the same as in Figure 2B, where it initially has the largest value $r(t_0)$ and then diminishes to zero as the battery discharges from t_0 to t_1. Thus, the initial V2G energy reserve can be derived as follows:

$$r(t_0) \coloneqq p_d(t_1 - t_0) = \frac{p_d(p_c T - E^{\text{target}})}{p_d + p_c}. \tag{5}$$

It should be noted that at this point, the initial V2G energy reserve $r(t_0)$ has become independent of the charging and discharging schedule; i.e., (5) holds in general scheduling cases.

4.1.2 General maximized discharge

Let $l(\cdot)$ denote the length of a Lebesgue-measurable subset of the set of real numbers $\mathbb{R}$. Then, in general cases, the maximum discharging period $\mathcal{T}_1$ is a Lebesgue-measurable subset of $[t_0, t_f]$ having the same length.

$$l(\mathcal{T}_1) = T_1 = t_1 - t_0 = \frac{p_c T - E^{\text{target}}}{p_d + p_c}. \tag{6}$$

Thus, for general maximal discharge cases, we can define the V2G energy reserve of an EV at time t as follows:

$$r(t) \coloneqq p_d l([t, t_f] \cap \mathcal{T}_1). \tag{7}$$

It is easy to verify that the initial energy reserve (5) derived for the second extreme case and the energy reserve (7) defined for general maximized discharge case are consistent. For general cases where an EV is not maximally discharged, $r(t)$ defined in Eq. 7 is still used to measure an EV's available V2G energy.

To deal with multiple EVs, let $r_i(t)$ denote the V2G energy reserve of EV i. By properly aggregating the individual V2G energy reserve $r_i(t)$, a certain $r(t)$-statistics-based charge park evaluation method can be developed. The differences between the $r(t)$-statistics-based evaluation method and general simulation-based evaluation method can be summarized as follows:

1. The $r(t)$-statistics-based evaluation aggregates the individual V2G energy reserve $r_i(t)$ and ignores distribution network constraints. Thus, the evaluation result reflects the V2G output potential instead of the accurate output capacity of the charge park. Since no simulation needs to be made, it is lightweight and suitable for early-stage planning, when the system parameters are still uncertain.
2. Simulation-based evaluation, on the other hand, needs to solve a scheduler optimization problem for a simulated charge demand scenario to compute the final metrics. It is more appropriate to use this method when a detailed system model is obtainable with readily available parameters.

In the following section, an $r(t)$-statistics-based evaluation method is developed, where the individual V2G energy reserves $r_i(t)$ for different EVs are aggregated according to the average import price (AIP) of the reserved energy $r_i(t)$. In Sections 5–6.3, on the other hand, a simulation-based evaluation method will be developed and used to compute an accurate estimation of the charge park V2G output capacity.

4.2 Case study: New York City working and recreational environment business charging

In this case study, an $r(t)$-statistics-based analysis was performed to evaluate the V2G output potential of New York City charge parks using the V2G energy reserve model (7), presented in Section 4.1, where each EV's V2G energy reserve was first computed and then aggregated by the AIP of the energy.

Specifically, a workplace charge park and a recreational environment charge park were considered in a near future New York City. The workplace charge park and the recreational environment charge park were assumed to have a total of 200 and 1,000 EVs parked on the designated date, respectively. In addition, the

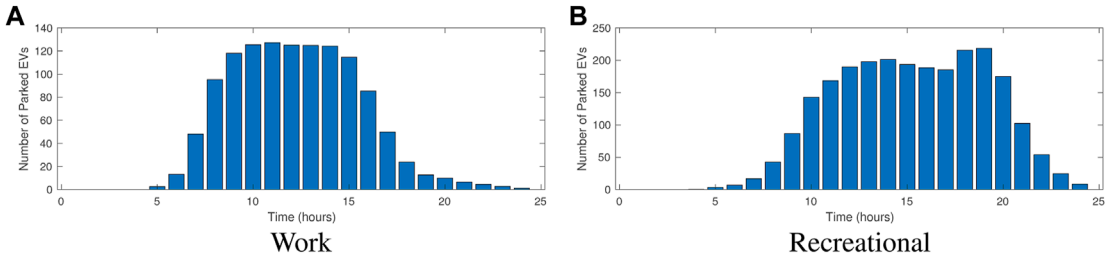

FIGURE 3
Parking lot occupancy prediction for a working environment (assuming a working day situation with a total of 200 daily parked vehicles) and a recreational environment (assuming a holiday situation with a total of 1,000 daily parked vehicles).

charge parks were assumed to adopt the service agreement, with $p_{ca} = 2.2$ kW and level 2 chargers of 6.6 kW (220V/30A). The discharging power was assumed to be the same as the charging power; thus, $p_d = p_c = 6.6$ kW.

4.2.1 Charge demand modeling

Considering the future adoption of larger battery sizes, it is assumed that 30% of the parked vehicles have battery capacities of 70 kWh, 50% have capacities of 90 kWh, and 20% have capacities of 110 kWh. The parking and charging patterns of the EV fleet were derived from the 2017 National Household Travel Survey (NHTS) data[1]. The parking lot occupancy situations for the two scenarios are shown in Figure 3.

As a current research practice, the SoC of an EV is estimated based on its daily travel distance. For example, in the work of Yunus et al. (2011), the SoC of an EV is derived using a synthesized vehicle's daily travel distance. Here, we use the arrival trip distance VMT_i of an EV i obtained from the 2017 NHTS database to derive the portion of SoC consumed by the trip $\delta s_i^{\mathrm{cur}} = \mathrm{VMT}_i \cdot e_m / B_i$ and then combine it with a generated SoC consumption $\delta s_i^{\mathrm{pre}} \sim U(0, 0.4)$ from a uniform distribution due to previous trips, with energy efficiency $e_m = 0.17$ kWh/km ≈ 0.27 kWh/miles. Each vehicle's SoC is then derived using

$$s_i = s_i^{\max} - \delta s_i^{\mathrm{cur}} - \delta s_i^{\mathrm{pre}}. \tag{8}$$

4.2.2 V2G energy reserve day-ahead analysis

Using the NYISO hourly day-ahead price data for New York City on 31 August 2018[2], the day-ahead analysis on the V2G energy reserve is performed for two peaks in the day-ahead price curve, i.e., 13:00 at 4.93¢/kWh and 16:00 at 4.95¢/kWh.

As shown in Figure 4, V2G energy is abundant at 13:00 since this time period connects peak hours and off-peak hours. On the other hand, at 16:00, there is still plenty of V2G energy in the recreational environment charge park compared to the workplace charge park since there are more parked EVs at this time, as shown in Figure 3. However, most of the EVs' V2G energy has higher AIP at 16:00 due to the average high electricity prices during the EVs' park time. In summary, V2G energy is most abundant at 13:00 in both workplace and recreational environment charging scenarios, while being healthier in the workplace charge park since most V2G energy has lower equivalent prices; i.e., the V2G energy is not only abundant but also cheaper (around 3.75¢/kWh and 4.05¢/kWh for workplace charge parks and greater than 4.1¢/kWh for recreational environment charge parks).

5 Day-ahead analysis-II: scheduler model and evaluation metrics

In this section, a dynamic evaluation framework is proposed to characterize the charge park's V2G output capability, using the 2017 NHTS data and a developed MILP-based scheduler. The evaluation intends to provide insights for the profit-seeking, decision-making process of the V2G service provider.

Figure 5 shows how the proposed framework may fit in the large picture of a V2G service provider. The main components of the evaluation framework are the MILP scheduler and the planning module, which serve for the profit-seeking process of the V2G service provider. The optimization solver used in this paper is the "intlinprog" solver in MATLAB, which is a powerful built-in solver specifically designed for solving MILP problems. The "intlinprog" solver utilizes an advanced branch-and-bound algorithm combined with linear programming relaxation to efficiently explore the feasible solution space and find an optimal solution. The model predictive controller (MPC) and the prediction parts are supposed to be implemented by the V2G service provider. It is worth mentioning that the MPC has already been applied in the PEVs operation studies Rahmani-Andebili and Fotuhi-Firuzabad (2017). Thus, the proposed framework can be readily connected to the current methodologies.

The purpose of the scheduler is to evaluate the V2G output capability of the charge park for every business day during the day-ahead planning, considering various constraints. The characterization of the charge park's V2G capability provides insights for the profit-seeking, decision-making process of the V2G service provider, described by the planning block. According to the characterization profiles, the V2G service provider determines the V2G output period, the V2G energy unit sale price, and the maximum power that can be supplied to its customers.

1 U.S. Department of Transportation and Federal Highway Administration. 2017 National Household Travel Survey. url: https://nhts.ornl.gov.

2 ENGIE Resources. Historical Data Reports. url: https://www.engieresources.com/historical-data.

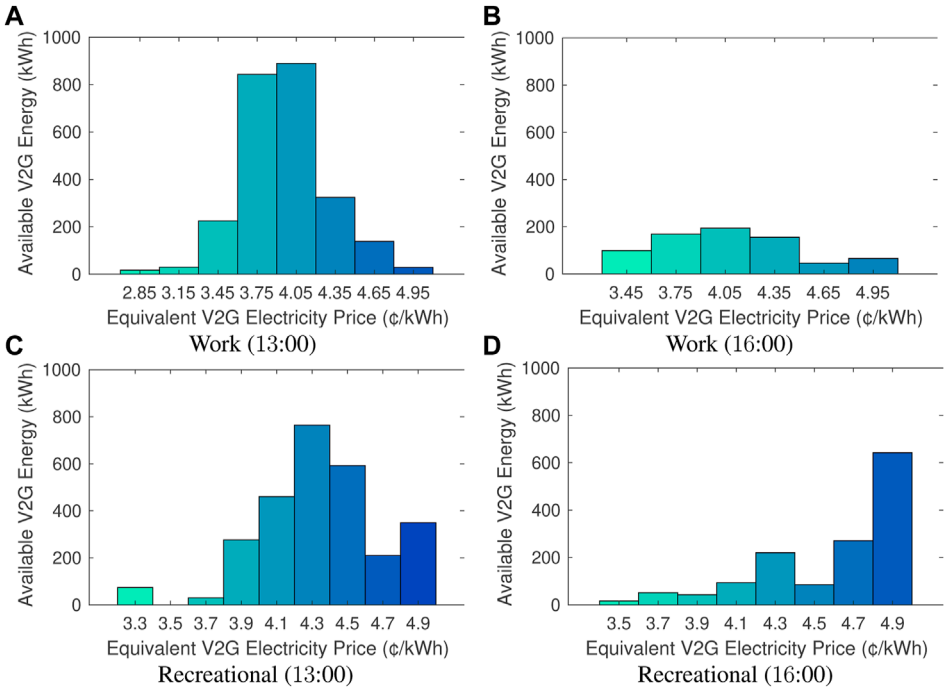

FIGURE 4
Available V2G energy reserve distribution over equivalent electricity prices (rounded) using varying battery capacities (30% of 35 kWh, 50% of 75 kWh, and 20% of 100 kWh).

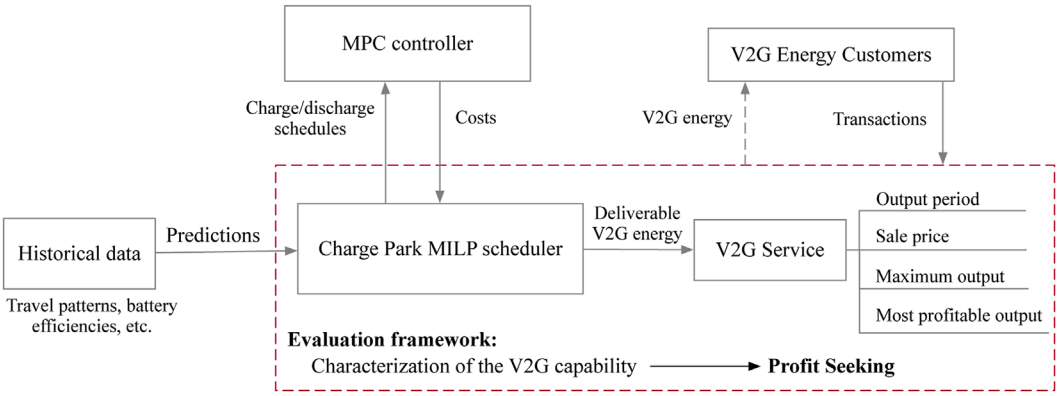

FIGURE 5
Evaluation framework for charge park V2G service capability.

Given the aforementioned information, the V2G customers then purchase power that the V2G service provider commits to supply.

5.1 System description and scheduler model

In Mouli et al. (2017), a mixed-integer linear programming-based scheduler is used to optimize the charging/discharging schedule. The main difference between the scheduler here and the one in the work of Mouli et al. (2017) is that the scheduler in the work of Mouli et al. (2017) optimizes a lumped objective of profit maximization and determines the V2G output commitment itself, which makes the higher-level service plan and contract decision-making impossible. In contrast, to characterize the charge park's V2G output capability for decision-making purposes, here, the V2G output period and power are given as parameters in the MILP problem, which aims to minimize the resulting electricity cost.

5.1.1 Charge park constraints

In the considered charge park, each charging station c connects to the grid via a DC/AC inverter of rated power P_c^{conv}. However, no PV source is considered here. Each charging station c can be multiplexed and connected with up to N_c^{conn} EVs. The connection pattern is indicated using $K_{v,t,c}$, where $K_{v,t,c} = 1$ means vehicle v is connected with charging station c at time t, and zero otherwise. Thus, it satisfies $\sum_{v=1}^{V} K_{v,t,c} \le N_c^{\text{conn}}, \forall c, t$. Furthermore, each charging station c has $N_c^{\text{ch}} \le N_c^{\text{conn}}$ number of isolated DC/DC converters (each with a rated power P_c^{EVr} for EV charging), which allows charging station c to simultaneously charge/discharge a maximum of N_c^{ch} connected EVs.

Let T_v^{a} and T_v^{d} denote the arrival and predicted departure times of EV v, respectively. Using an activation indicator $a_{v,t}^{\text{act}}$, the following constraints specify when EVs can be actively charging/discharging.

$$a_{v,t}^{\text{act}} \in \{0,1\}, \quad \forall v, t, \tag{9}$$

$$a_{v,t}^{\text{act}} = 0, \quad \forall v \text{ and } t \le T_v^{\text{a}}, \tag{10}$$

$$a_{v,t}^{\text{act}} = 0, \quad \forall v \text{ and } t \ge T_v^{\text{d}}, \tag{11}$$

$$\sum_{v=1}^{V} a_{v,t}^{\text{act}} K_{v,t,c} \le N_c^{\text{ch}}. \quad \forall t, c. \tag{12}$$

The V2G activity of each EV is indicated by $a_{v,t}^{\text{v2g}}$, such that at time t, EV v is charging if $a_{v,t}^{\text{v2g}} = 0$ and is discharging if $a_{v,t}^{\text{v2g}} = 1$. The rated powers for charging and discharging at converter c are assumed to be the same and are denoted as P_c^{EVr}. The following constraints specify the V2G operation power limits.

$$x_{v,t}^{e+}, x_{v,t}^{e-} \le P_c^{\text{EVr}} a_{v,t}^{\text{act}}, \quad \forall v, t, c \text{ with } K_{v,t,c} = 1, \tag{13}$$

$$x_{v,t}^{e+} \le P_c^{\text{EVr}} \left(1 - a_{v,t}^{\text{v2g}}\right), \quad \forall v, t, \tag{14}$$

$$x_{v,t}^{e-} \le P_c^{\text{EVr}} a_{v,t}^{\text{v2g}}, \quad \forall v, t, \tag{15}$$

$$a_{v,t}^{\text{v2g}} \in \{0,1\}. \quad \forall v, t. \tag{16}$$

Eqs 17–21 are constraints for battery energy evolution. Here, the constant B_v^{a} denotes the arrival battery energy of EV v, $b_{v,t}$ denotes the EV battery energy as a decision variable for a different time t, and E_v^{target} is the charge demand given by (1) for EV v. It is assumed that at every time interval with length ΔT, an EV is either charging with efficiency η_v^+ or discharging with efficiency η_v^-, and no switching occurs during either time interval.

$$b_{v,t} = B_v^a, \quad \forall v \text{ and } t = T_v^{\text{a}}, \tag{17}$$

$$b_{v,t} \le b_v^a + E_v^{\text{target}}, \quad \forall v \text{ and } t = T_v^{\text{d}}, \tag{18}$$

$$b_{v,t+1} = b_{v,t} + \Delta T\left(x_{v,t}^{e+}\eta_v^+ - x_{v,t}^{e-}/\eta_v^-\right), \quad \forall t, v, \tag{19}$$

$$b_{v,t} \ge B_v^{\min}, \quad \forall t, v, \tag{20}$$

$$b_{v,t} \le B_v^{\max}. \quad \forall t, v. \tag{21}$$

Eqs 22–24 are the power exchange constraints for each charging station. Each charging station c draws power $p_{c,t}^{\text{draw}}$ from or feeds power $p_{c,t}^{\text{feed}}$ to the charge park AC grid, limited by the rated power P_c^{conv} of its DC/AC inverter port. A binary variable $a_{c,t}^{\text{feed}}$ is used to indicate whether a charging station c is drawing power from or feeding power to the charge park at time t.

$$\left(p_{c,t}^{\text{draw}} + \sum_{v=1}^{V}\left(x_{v,t}^{e-}K_{v,t,c}\right)\right)\eta_c^{\text{conv}} = \left(p_{c,t}^{\text{feed}} + \sum_{v=1}^{V}\left(x_{v,t}^{e+}K_{v,t,c}\right)\right)/\eta_c^{\text{conv}}, \quad \forall c, t, \tag{22}$$

$$p_{c,t}^{\text{draw}} \le P_c^{\text{conv}}\left(1 - a_{c,t}^{\text{feed}}\right), \quad \forall c, t, \tag{23}$$

$$p_{c,t}^{\text{feed}} \le P_c^{\text{conv}}\left(a_{c,t}^{\text{feed}}\right). \quad \forall c, t. \tag{24}$$

Eqs 25–27 are constraints for the total power imported from or exported to the distribution grid by the charge park. The imported power p_t^{imp} and the exported power p_t^{exp} are limited by the distribution import and export power limits $P_t^{\text{DN+}}$ and $P_t^{\text{DN-}}$, respectively.

$$\sum_{c=1}^{C}\left(p_{c,t}^{\text{draw}} - p_{c,t}^{\text{feed}}\right) = p_t^{\text{imp}} - p_t^{\text{exp}}, \quad \forall t, \tag{25}$$

$$p_t^{\text{imp}} \le P_t^{\text{DN+}}\left(1 - a_t^{\text{exp}}\right), \quad \forall t, \tag{26}$$

$$p_t^{\text{exp}} \le P_t^{\text{DN-}} a_t^{\text{exp}}. \quad \forall t. \tag{27}$$

5.1.2 Decision constraints

According to the service agreement (ref. Eq. 1), the charge demand of EV v is given by

$$E_v^{\text{target}} = \min\left\{p_{\text{ca}} T_v, B_v^{\max} - B_v^{\text{a}}\right\}, \tag{28}$$

where $T_v = T_v^{\text{d}} - T_v^{\text{a}}$ is the predicted dwell time of EV v, $B_v^{\max}$ is the maximum battery energy of EV v, and p_{ca} is the average charging power guaranteed by the policy.

The following constraint describes the V2G output demand that needs to be satisfied by the charge park.

$$p_t^{\text{exp}} >= P^{\text{v2g}}, \quad \text{for } t \in \mathcal{T}^{\text{v2g}}, \tag{29}$$

where $\mathcal{T}^{\text{v2g}}$ denotes the V2G output time period, i.e., the set of time instants where V2G service is required, and P^{v2g} is the committed V2G output power.

5.1.3 Optimization objective

The objective of the scheduler is to minimize the electricity cost plus the penalty for failing to satisfy the EV charge demand. Let e^{nff} denote the EV charge-demand-not-fulfilled (CDnf) and c^{imp} denote the imported electricity cost (ECost). They are given by

$$e^{\text{nff}} = \sum_{v=1}^{V}\left(B_v^{\text{a}} + E_v^{\text{target}} - b_{T_v^{\text{d}},v}\right), \tag{30}$$

$$c^{\text{imp}} = \Delta T \sum_{t=1}^{T} C_t^{\text{buy}} p_t^{\text{imp}}, \tag{31}$$

where C_t^{buy} is the grid electricity import price at time t. Here, $\Delta T = 15$ mins, and $T = (60/15) \times 24 = 96$.

The optimization objective can be represented as follows:

$$\text{Min} \quad f = C^{\text{p}} e^{\text{nff}} + c^{\text{imp}}, \tag{32}$$

where C^{p} is the penalty coefficient for failing to satisfy the charge demand. For small C^{p}, an optimal solution may have a non-zero e^{nff}, sacrificing EV charge demand satisfaction for lower imported electricity cost c^{imp}. By adjusting the value of C^{p}, the charge park system operator controls how strictly the scheduler satisfies the EV charge demand. Here, C^{p} is set to be very large compared to e^{nff} and c^{imp} so that the reduction of CDnf e^{nff} will always be prioritized over the reduction of ECost c^{imp}. The variables of the optimization problem are summarized in the nomenclature at C-2 "Optimization variables."

5.2 Evaluation measures

Let $e^{\text{nff}}(p)$ and $c^{\text{imp}}(p)$ denote the CDnf (30) and ECost (31), respectively, as functions of the V2G output power $P^{\text{v2g}} = p$. To study the dependence of the optimization solution on the V2G output power P^{v2g} for a fixed output time period $\mathcal{T}^{\text{v2g}}$, extra evaluation measures are introduced as follows.

5.2.1 V2G output power capacity

The V2G output power capacity $p_{\text{cap}}^{\text{v2g}}$ is defined as the maximum output power p such that CDnf can be kept as zero:

$$p_{\text{cap}}^{\text{v2g}} = \max\left\{p \in [0, P_{\text{DN}-}] : e^{\text{nff}}(p) = 0\right\}. \tag{33}$$

5.2.2 V2G service cost and profit

Here, several common evaluation measures in economics are defined for the study of the V2G service. It is worth pointing out that the "unit costs" and "marginal costs" defined as follows are computed with respect to the supplied energy $p|\mathcal{T}^{\text{v2g}}|$ instead of the output power p so that it is easier to compare them with the electricity market price.

- V2G energy average unit cost:

$$C_{\text{a}}^{\text{v2g}}(p) = \frac{c^{\text{imp}}(p) - c^{\text{imp}}(0)}{p|\mathcal{T}^{\text{v2g}}|}, \tag{34}$$

  where $|\mathcal{T}^{\text{v2g}}|$ denotes the length of the V2G output period $\mathcal{T}$.
- V2G energy incremental unit cost:

$$C_{\delta p}^{\text{v2g}}(p) = \frac{\delta c^{\text{imp}}(p)}{\delta p|\mathcal{T}^{\text{v2g}}|} = \frac{c^{\text{imp}}(p+\delta p) - c^{\text{imp}}(p)}{\delta p|\mathcal{T}^{\text{v2g}}|}, \tag{35}$$

  for some evaluation interval δp.
- V2G energy marginal cost:

$$C^{\text{v2g}}(p) = \frac{\mathrm{d}c^{\text{imp}}(p)}{\mathrm{d}p|\mathcal{T}^{\text{v2g}}|}. \tag{36}$$

TABLE 1 Simulation parameters.

Symbol	Description	Value
p_{d}	Rated discharge power for an EV	6.6 kW
p_{c}	Rated charge power for an EV	6.6 kW
p_{ca}	EV average charge power	2.2 kW
ΔT	Time step length for the scheduler	15 mins
$P_{\text{DN}+}$	Distribution import power limits	200 kW
$P_{\text{DN}-}$	Distribution export power limits	200 kW

- Total profit of the V2G service for the scheduling day, ignoring investment and maintenance cost for the charge park's facilities:

$$\begin{aligned}\text{Pr}(p) &= S^{\text{v2g}} p|\mathcal{T}^{\text{v2g}}| - \left(c^{\text{imp}}(p) - c^{\text{imp}}(0)\right) \\ &= \left(S^{\text{v2g}} - C_{\text{a}}^{\text{v2g}}(p)\right) p|\mathcal{T}^{\text{v2g}}|,\end{aligned} \tag{37}$$

  where S^{v2g} is the unit sale price of the V2G energy for the supply period $\mathcal{T}^{\text{v2g}}$.
- V2G service marginal profit:

$$\text{MP}(p) = \frac{\mathrm{dPr}(p)}{\mathrm{d}p|\mathcal{T}^{\text{v2g}}|} = S^{\text{v2g}} - C^{\text{v2g}}(p). \tag{38}$$

6 Day-ahead analysis-II: evaluation methods and profit maximization

This section presents a theoretical basis for the characterization of charge park V2G service output capability.

6.1 General characteristics of imported electricity cost and charge-demand-not-fulfilled

Here, distribution network limits $P_{\text{DN}+} = P_{\text{DN}-} = 200\text{kW}$ are used. Furthermore, all the simulation parameters are listed in Table 1. Currently, battery charging and discharging efficiencies η_v^+ and η_v^- usually range from 0.85 to 0.9, and the charging station converter efficiency η_c^{conv} ranges from 0.95 to 0.975. These values are expected to increase, and their variance is expected to decrease in the future due to technological advancement. Thus, in this research, the following assumption of uniform efficiency parameters is used to study the characteristics of the V2G service.

Assumption 1. *A so-called "uniform efficiency setting" is considered, where all battery charging and discharging efficiencies take the same value, i.e., $\eta_v^+ = \eta_v^- = \eta^{\text{ev}}$ for all v, and all charging station converter efficiencies take the same value, i.e., $\eta_c^{\text{conv}} = \eta^{\text{conv}}$ for all c. The following are two specific efficiency settings under this assumption:*

1. *"Ideal efficiency" refers to when $\eta^{\text{ev}} = \eta^{\text{conv}} = 1$.*
2. *"Uniform realistic efficiency" refers to when η^{ev} and η^{conv} take fixed positive values less than one. In the simulations of this paper, $\eta^{\text{ev}} = 0.9$ and $\eta^{\text{conv}} = 0.975$.*

The following proposition describes the behaviors of ECost $c^{\text{imp}}(p)$ and CDnf $e^{\text{nff}}(p)$.

Proposition 1. *Suppose that Assumption* 1 *holds* $\eta_v^+ = \eta_v^- = \eta^{\text{ev}}$ *for all* v *and* $\eta_c^{\text{conv}} = \eta^{\text{conv}}$ *for all* c. *If the CDnf penalty* C^{p} *is large enough and* $e^{\text{nff}}(0) = 0$, *there exists a V2G output power capacity* $p_{\text{cap}}^{\text{v2g}} \geq 0$ *such that the CDnf* e^{nff} (30) *and ECost* c^{imp} (31) *satisfy the following properties:*

1. *The CDnf* $e^{\text{nff}}(p)$, *as a function of the V2G output power* p, *satisfies* $e^{\text{nff}}(p) = 0$ *(all charge demand met) for* $p \leq p_{\text{cap}}^{\text{v2g}}$, *and*

$$\frac{\mathrm{d}e^{\text{nff}}(p)}{\mathrm{d}p|\mathcal{T}^{\text{v2g}}|} = \frac{1}{\eta^{\text{ev}}(\eta^{\text{conv}})^2}, \tag{39}$$

   for $p > p_{\text{cap}}^{\text{v2g}}$.
2. *As long as* $C_t^{\text{buy}} > 0$ *for* $t \in \mathcal{T}^{\text{v2g}}$ *(buying price is positive), the ECost* $c^{\text{imp}}(p)$, *as a function of the V2G output power* p, *strictly monotonically increases for* $p < p_{\text{cap}}^{\text{v2g}}$, *and* $c^{\text{imp}}(p) = c^{\text{imp}}\left(p_{\text{cap}}^{\text{v2g}}\right)$ *for all* $p > p_{\text{cap}}^{\text{v2g}}$.

Proof: When $p \leq p_{\text{cap}}^{\text{v2g}}$, the output demand $p|\mathcal{T}^{\text{v2g}}|$ can be satisfied by importing extra energy from the grid during off-peak hours, storing in EV batteries, and discharging during the output period. However, when $p > p_{\text{cap}}^{\text{v2g}}$, $p - p_{\text{cap}}^{\text{v2g}}$ is the extra V2G output demand that cannot be satisfied by importing extra energy from the grid and is, thus, compensated by discharging extra EV battery energy, which results in increased CDnf $e^{\text{nff}}(p)$. The amount of EV battery energy to be discharged is increased due to both the (uniform) EV battery efficiency η^{ev} and the converter efficiency η^{conv}. The converter efficiency η^{conv} considered here applies twice, as shown in Eq. 22, thus resulting in Eq. 39 as the slope of CDnf when $p > p_{\text{cap}}^{\text{v2g}}$.

The ECost $c^{\text{imp}}(p)$ for $p = 0$ is the electricity cost for charging EV batteries only. Since for $p \leq p_{\text{cap}}^{\text{v2g}}$, the output demand is satisfied by importing extra energy from the grid during off-peak hours, the electricity cost also increases. When $p > p_{\text{cap}}^{\text{v2g}}$, no extra energy is imported from the grid, thus resulting in $c^{\text{imp}}(p) = c^{\text{imp}}\left(p_{\text{cap}}^{\text{v2g}}\right)$ for all $p > p_{\text{cap}}^{\text{v2g}}$.

Verification of this proposition will be carried out in Section 6.2. Since the CDnf penalty C^{p} is very large, reducing the value of $e^{\text{nff}}(p)$ is of the highest priority in the solution of Eqs 9–32. When $p \leq p^{\text{v2g}}$, the V2G output demand $p|\mathcal{T}^{\text{v2g}}|$ can be satisfied by importing more electricity in non-V2G hours. Thus, $c^{\text{imp}}(p)$ is strictly $\left(C_t^{\text{buy}} > 0\right)$ monotonically increasing for $p < p^{\text{v2g}}$, keeping $e^{\text{nff}}(p) = 0$ for $p < p^{\text{v2g}}$. When $p > p^{\text{v2g}}$, some EV charge demand has to be sacrificed in order to meet the V2G output demand. Thus, the CDnf is strictly monotonically increasing for $p > p^{\text{v2g}}$. In addition, as excessive V2G output energy $\left(p - p_{\text{cap}}^{\text{v2g}}\right)|\mathcal{T}^{\text{v2g}}|$ comes from the sacrificed charge demand $e^{\text{nff}}(p) > 0$, which is affected by the efficiency η^{ev} once and η^{conv} twice according to (9)–(32), $\left(p - p_{\text{cap}}^{\text{v2g}}\right)|\mathcal{T}^{\text{v2g}}| = e^{\text{nff}}(p)\eta^{\text{ev}}(\eta^{\text{conv}})^2$ holds.

6.1.1 Electricity cost under time-of-use pricing

Currently, two-price and three-price time-of-use (TOU) plans are the most common pricing plans for business users. In California, all commercial, industrial, and agricultural customers are required to be on a TOU plan, as TOU pricing encourages the most efficient use of the system and can reduce the overall costs for both the utility and customers. The on-peak electricity price C_2^{TOU} can be 20–200% higher than the off-peak electricity price C_1^{TOU}, depending on the region, utility, and the type of customers.

As shown in Figure 6, each day is divided into an on-peak period $\mathcal{T}_{\text{peak}}^{\text{TOU}}$ and an off-peak period $\mathcal{T}_{\text{off-peak}}^{\text{TOU}}$. The electricity price is $C_t^{\text{buy}} = C_1^{\text{TOU}}$ for off-peak hours $t \in \mathcal{T}_{\text{off-peak}}^{\text{TOU}}$ and $C_t^{\text{buy}} = C_2^{\text{TOU}}$ for peak hours $t \in \mathcal{T}_{\text{peak}}^{\text{TOU}}$.

6.2 Evaluation with ideal efficiency parameters

In this section, the charge park V2G service was evaluated under Assumption 1 with the ideal efficiency setting. The working day workplace charging environment in Section 4.2 was considered. Specifically, the charge park had a total of 200 parked vehicles in the simulated day with workplace activity patterns, and the diverse battery capacity setting was used.

6.2.1 Imported electricity cost

The following proposition describes the characteristics of the scheduled day electricity cost $c^{\text{imp}}(p)$ as a function of the output power $P^{\text{v2g}} = p$ under a two-price TOU plan.

Proposition 2. *Assuming a two-price TOU plan and the ideal efficiency setting (Assumption* 1 *Setting* 1*), the total ECost* c^{imp} *can be characterized as a three-piece piecewise linear function of the output power* p, *as follows:*

$$c^{\text{imp}}(p) = \begin{cases} c^{\text{imp}}(0) + C_1^{\text{TOU}}|\mathcal{T}^{\text{v2g}}|p, & p \leq p_{\text{TOU}}^{\text{v2g}}, \\ c^{\text{imp}}\left(p_{\text{TOU}}^{\text{v2g}}\right) & \\ \quad + C_2^{\text{TOU}}|\mathcal{T}^{\text{v2g}}|\left(p - p_{\text{TOU}}^{\text{v2g}}\right), & p_{\text{TOU}}^{\text{v2g}} < p \leq p_{\text{cap}}^{\text{v2g}}, \\ c^{\text{imp}}\left(p_{\text{cap}}^{\text{v2g}}\right), & p_{\text{cap}}^{\text{v2g}} < p \leq P_{\text{DN}-}, \end{cases} \tag{40}$$

where $p_{\text{TOU}}^{\text{v2g}}$ *is the V2G output power threshold at which the marginal cost changes from* C_1^{TOU} *to* C_2^{TOU}.

Proof: It should be noted that system (9)–(32) is essentially mixed-integer linear programming; thus, $c^{\text{imp}}(p)$ must be linear. Since system (9)–(32) was designed to prioritize charging EVs in off-peak hours (with electricity price C_1^{TOU}), when $p \leq p_{\text{cap}}^{\text{v2g}}$, $c^{\text{imp}}(p)$ can only first increase with slope $C_1^{\text{TOU}}|\mathcal{T}^{\text{v2g}}|$ and then increase with slope $C_2^{\text{TOU}}|\mathcal{T}^{\text{v2g}}| > C_1^{\text{TOU}}|\mathcal{T}^{\text{v2g}}|$. Finally, ECost $c^{\text{imp}}(p)$ for $p > p_{\text{cap}}^{\text{v2g}}$ is given by Proposition 1.

Figures 7–8 show the variations of electricity cost $c^{\text{imp}}(p)$, CDnf $e^{\text{nff}}(p)$, and V2G energy marginal cost $C^{\text{v2g}}(p)$ with respect to the V2G output power $P^{\text{v2g}} = p \in [0, P_{\text{DN}-}]$. The V2G energy marginal cost $C^{\text{v2g}}(p)$ is approximated using V2G energy incremental unit cost $C_{\delta p}^{\text{v2g}}$ defined in Eq. 35 with $\delta p = 10$kW.

Figure 7 demonstrates the results where part of the non-V2G hours are on-peak; specifically, $\mathcal{T}^{\text{v2g}} = [13{:}00, 15{:}00]$ and $\mathcal{T}_{\text{peak}}^{\text{TOU}} = [12{:}00, 16{:}00]$. In this case, $p_{\text{cap}}^{\text{v2g}} = P_{\text{DN}-} = 200$kW; thus, $e^{\text{nff}}(p) = 0$ for $p \in [0, P_{\text{DN}-}]$. For Figure 7, the following steps are taken to verify Proposition 2. Assuming that Proposition 2 is true, with the knowledge of $c^{\text{imp}}(p)$ at $p = 0$ and $p = p_{\text{cap}}^{\text{v2g}}$, solving (41) and (42) leads to $p_{\text{TOU}}^{\text{v2g}} = 90.8566$kW:

$$c^{\text{imp}}\left(p_{\text{TOU}}^{\text{v2g}}\right) - c^{\text{imp}}(0) = C_1^{\text{TOU}}|\mathcal{T}^{\text{v2g}}|p_{\text{TOU}}^{\text{v2g}}, \tag{41}$$

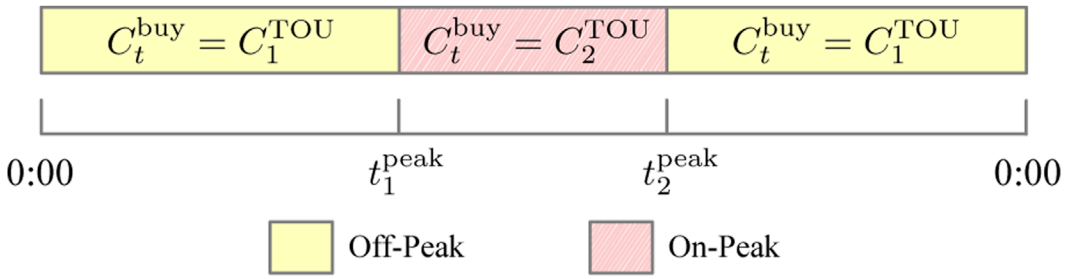

FIGURE 6
Time-of-use pricing plan with off-peak and on-peak levels, where the on-peak time period is $\mathcal{T}_{\text{peak}}^{\text{TOU}} = \left[t_1^{\text{peak}}, t_2^{\text{peak}}\right]$. Grid electricity unit price is C_1^{TOU} for off-peak hours and C_2^{TOU} for on-peak hours.

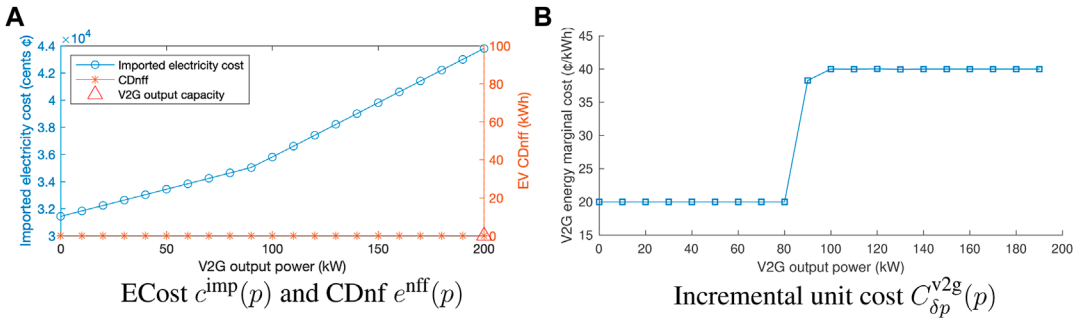

FIGURE 7
ECost $c^{\text{imp}}(p)$ and V2G energy marginal cost $C^{\text{v2g}}(p)$ (approximated by the incremental unit cost $C_{\delta p}^{\text{v2g}}(p)$ with δp =10 kW) when using the ideal efficiency setting with the output period $\mathcal{T}^{\text{v2g}}$ = [13:00,15:00] and on-peak hours $\mathcal{T}_{\text{peak}}^{\text{TOU}}$ = [12:00,16:00].

$$c^{\text{imp}}\left(p_{\text{cap}}^{\text{v2g}}\right) - c^{\text{imp}}\left(p_{\text{TOU}}^{\text{v2g}}\right) = C_2^{\text{TOU}}|\mathcal{T}^{\text{v2g}}|\left(p_{\text{cap}}^{\text{v2g}} - p_{\text{TOU}}^{\text{v2g}}\right). \quad (42)$$

Then, the ECost $c^{\text{imp}}(p_{\text{TOU}}^{\text{v2g}})$ is evaluated by solving (9)–(32) with $P^{\text{v2g}} = p_{\text{TOU}}^{\text{v2g}} = 90.8566\text{kW}$. In this case, it yields $c^{\text{imp}}\left(p_{\text{TOU}}^{\text{v2g}}\right) = 3.5074\text{E}+04¢$. Finally, the evaluated cost $c^{\text{imp}}\left(p_{\text{TOU}}^{\text{v2g}}\right)$ is substituted in Eqs 41, 42, and the computation shows that the equations hold. Thus, the aforementioned steps verify Proposition 2.

Corollary 1. *Under the two-price TOU plan and the ideal efficiency scenario (Assumption 1 Setting 1), the V2G output power threshold* $p_{\text{TOU}}^{\text{v2g}}$ *can be computed using*

$$p_{\text{TOU}}^{\text{v2g}} = \frac{C_2^{\text{TOU}} p_{\text{cap}}^{\text{v2g}} - \left(c^{\text{imp}}\left(p_{\text{cap}}^{\text{v2g}}\right) - c^{\text{imp}}(0)\right)/|\mathcal{T}^{\text{v2g}}|}{C_2^{\text{TOU}} - C_1^{\text{TOU}}}, \quad (43)$$

by evaluating $c^{\text{imp}}(p)$ *at* $p = 0$ *and* $p = p_{\text{cap}}^{\text{v2g}}$.

Proof: The result is immediate from Eqs 41, 42.

Then, Figure 8 demonstrates the characteristics of the V2G service with a long V2G output period $\mathcal{T}^{\text{v2g}}$ = [13:00, 16:00]. In this case, the V2G output power capacity is smaller than the distributed network limit, i.e., $p_{\text{cap}}^{\text{v2g}} = 127.24\text{kW} < P_{\text{DN}-} = 200\text{kW}$. In accordance with Propositions 1 and 2, as shown in Figure 8, ECost $c^{\text{imp}}(p) = c^{\text{imp}}\left(p_{\text{cap}}^{\text{v2g}}\right)$ for $p \in \left(p_{\text{cap}}^{\text{v2g}}, P_{\text{DN}-}\right]$, and the characteristics of CDnf $e^{\text{nff}}(p)$ shown in Figures 8A, C also verify (39) in Proposition 1, since $\eta^{\text{ev}} = \eta^{\text{conv}} = 1$ in ideal efficiency setting. In the following section, $p_{\text{TOU}}^{\text{v2g}}$ will be shown to be the optimal output power for the ideal efficiency scenario.

6.2.2 Profit maximization

As shown in Eq. 37, the profit $\Pr(p)$ depends on the V2G energy unit sale price S^{v2g}, output power p for period $\mathcal{T}^{\text{v2g}}$, and the electricity import cost $c^{\text{imp}}(p)$. The main considerations regarding the determination of sale price S^{v2g} are summarized in the following two points:

1. In order to gain a competitive edge over the grid electricity provider, the unit sale price of the V2G energy S^{v2g} needs to be smaller than the electricity unit price C_t^{buy} for buying electricity from the grid during period $\mathcal{T}^{\text{v2g}}$, i.e., $S^{\text{v2g}} < C_t^{\text{buy}}$ for $t \in \mathcal{T}^{\text{v2g}}$.
2. On the other hand, to gain profit by providing a V2G service, the V2G energy unit sale price S^{v2g} needs to be greater than the V2G energy average unit cost $C_{\text{a}}^{\text{v2g}}(p)$, i.e., $S^{\text{v2g}} > C_{\text{a}}^{\text{v2g}}(p)$.

Thus, reducing the average unit cost $C_{\text{a}}^{\text{v2g}}(p)$ is essential to guarantee a good sale price S^{v2g} and maximize the profit.

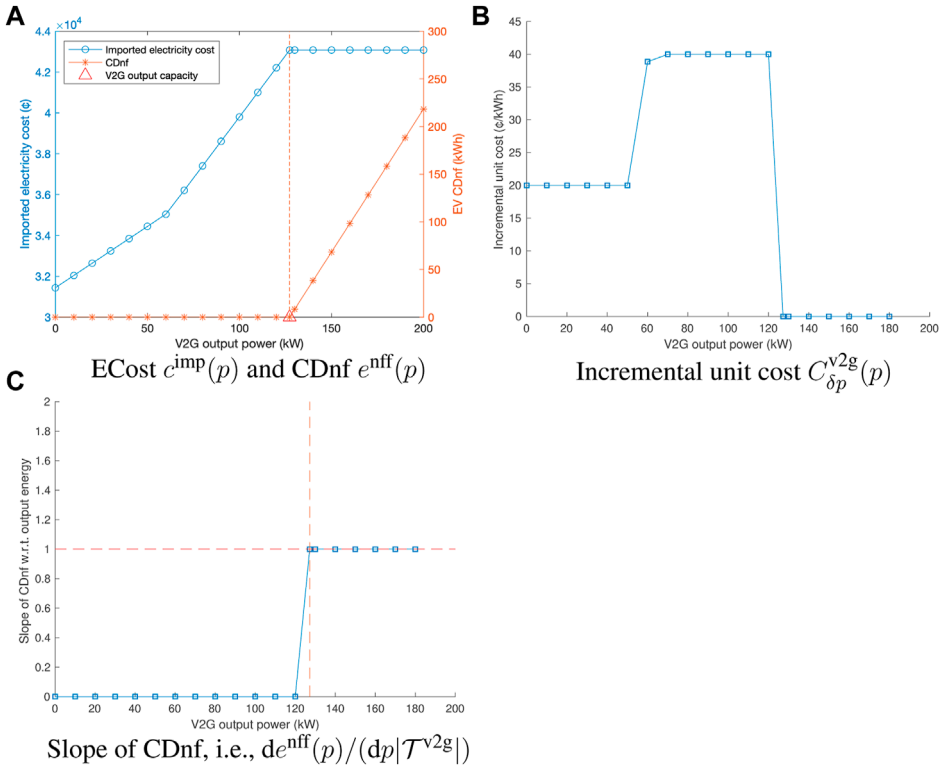

FIGURE 8
ECost $c^{\text{imp}}(p)$ and CDnf $e^{\text{nff}}(p)$, V2G energy marginal cost $C^{\text{v2g}}(p)$ (approximated by the incremental unit cost $C^{\text{v2g}}_{\delta p}(p)$ with δp =10 kW), and the slope of CDnf (w.r.t. output energy) $\mathrm{d}e^{\text{nff}}(p)/(\mathrm{d}p|\mathcal{T}^{\text{v2g}}|)$ when using the ideal efficiency setting with the output period $\mathcal{T}^{\text{v2g}}$ = [13:00,16:00] and $\mathcal{T}^{\text{TOU}}_{\text{peak}}$ = [12:00,16:00].

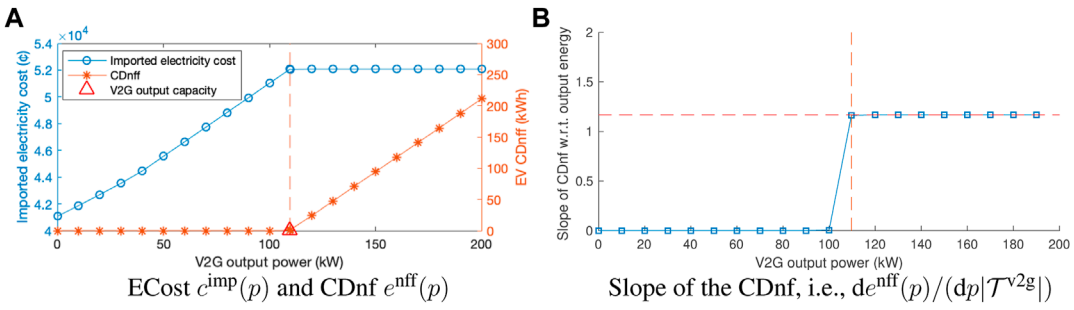

FIGURE 9
Evaluation results for $\mathcal{T}^{\text{v2g}}$ = [12:00,14:00] and $\mathcal{T}^{\text{TOU}}_{\text{peak}}$ = [12:00,16:00], using the uniform realistic efficiency setting.

For the ideal efficiency scenario with the two-price TOU plan, the following corollary gives a range of feasible sale prices S^{v2g} and the output power p that maximize the profit $\Pr(p)$ defined in Eq. 37.

Corollary 2. *Under the two-price TOU plan and considering the ideal efficiency scenario (Assumption* 1 *Setting 1), if* S^{v2g} *is chosen such that* $C^{\text{TOU}}_1 < S^{\text{v2g}} < C^{\text{TOU}}_2$, *the profit* $\Pr(p)$ *is maximized at* $p = p^{\text{v2g}}_{\text{TOU}}$.

Proof: First, $S^{\text{v2g}} > C^{\text{TOU}}_1$ implies $S^{\text{v2g}} > C^{\text{v2g}}_{\text{a}}(p)$ for any $p \le p^{\text{v2g}}_{\text{TOU}}$. Since $C^{\text{buy}}_t = C^{\text{TOU}}_2$ for $t \in T^{\text{v2g}}$, the sale price condition $C^{\text{v2g}}_{\text{a}}(p) < S^{\text{v2g}} < C^{\text{buy}}_t$ is satisfied at $p = p^{\text{v2g}}_{\text{TOU}}$.

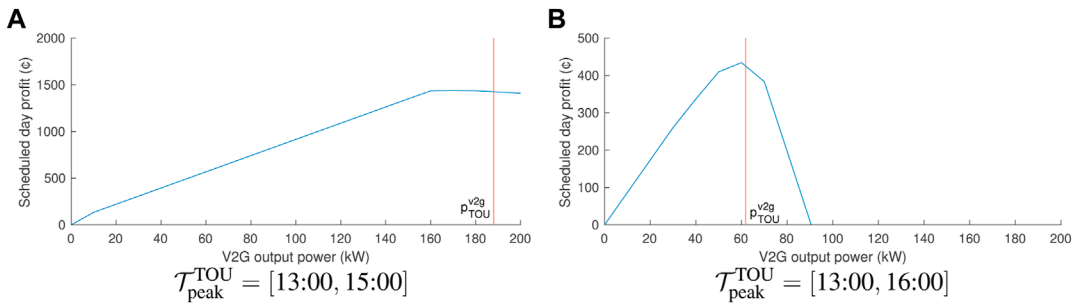

FIGURE 10
Profit Pr(p) for the output period $\mathcal{T}^{\text{v2g}}$ = [13:00,14:00] and different TOU peak period scenarios, with sale price $S^{\text{v2g}} = C_2^{\text{TOU}} - 4$¢/kWh, using the uniform realistic efficiencies.

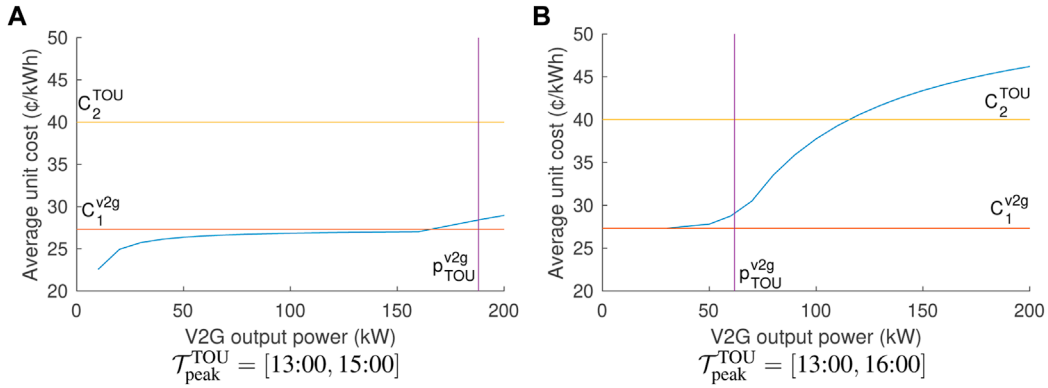

FIGURE 11
V2G energy average unit cost C_a^{v2g} for the output period $\mathcal{T}^{\text{v2g}}$ = [13:00,14:00] and different TOU peak period scenarios, using the uniform realistic efficiencies.

Next, from Proposition 2, the V2G energy marginal cost (36) for the ECost $c^{\text{imp}}(p)$ can be given as follows:

$$C^{\text{v2g}}(p) = \begin{cases} C_1^{\text{TOU}}, & p < p_{\text{TOU}}^{\text{v2g}}, \\ C_2^{\text{TOU}}, & p_{\text{TOU}}^{\text{v2g}} < p < p_{\text{cap}}^{\text{v2g}}. \end{cases} \tag{44}$$

Thus, the marginal profit (38) satisfies $\text{MP}(p) = S^{\text{v2g}} - C_1^{\text{TOU}} > 0$ for $p < p_{\text{TOU}}^{\text{v2g}}$ and $\text{MP}(p) = S^{\text{v2g}} - C_2^{\text{TOU}} < 0$ for $p_{\text{TOU}}^{\text{v2g}} < p < p_{\text{cap}}^{\text{v2g}}$. Therefore, the profit Pr(p) (37) is maximized at $p = p_{\text{TOU}}^{\text{v2g}}$.

6.3 Evaluation with the uniform realistic efficiency setting

6.3.1 Efficiency parameters

In this section, the characteristics of the ECost $c^{\text{imp}}(p)$ when using the uniform realistic efficiency setting (Assumption 1 Setting 2) are demonstrated. Other configurations for simulation are the same as in Section 6.2.

Figure 9 shows the evaluation results when $\mathcal{T}^{\text{v2g}} = [12{:}00, 14{:}00]$ and $\mathcal{T}^{\text{TOU}}_{\text{peak}} = [12{:}00, 16{:}00]$. It can be seen from Figure 9A that the overall ECost $c^{\text{imp}}(p)$ and CDnf $e^{\text{nff}}(p)$ profiles are similar to when using the ideal efficiency setting. For closer observation, Figure 9B shows the slope of CDnf, i.e., $\text{d}e^{\text{nff}}(p)/(\text{d}p|\mathcal{T}^{\text{v2g}}|)$. According to Proposition 1, $\text{d}e^{\text{nff}}(p)/(\text{d}p|\mathcal{T}^{\text{v2g}}|) \approx 1.1688$, which is verified in Figure 9B.

When using the uniform realistic efficiency configuration, according to Proposition 1, the V2G output capacity $p_{\text{cap}}^{\text{v2g}}$ can be computed with

$$p_{\text{cap}}^{\text{v2g}} = p - \frac{e^{\text{nff}}(p)\,\eta^{ev}(\eta^{\text{conv}})^2}{|\mathcal{T}^{\text{v2g}}|}, \tag{45}$$

for any $p \geq p_{\text{cap}}^{\text{v2g}}$. Thus, assuming that $P_{\text{DN}-}$ is a feasible solution of Eqs 9–32, the V2G output capacity $p_{\text{cap}}^{\text{v2g}}$ can be computed using Eq. 45 with $p = P_{\text{DN}-}$.

In addition, with a uniform realistic efficiency setting, the characteristic marginal cost values are defined as follows:

$$C_1^{\text{v2g}} = C_1^{\text{TOU}} / \left((\eta^{\text{ev}})^2 (\eta^{\text{conv}})^4\right) \tag{46}$$

and

$$C_2^{\text{v2g}} = C_2^{\text{TOU}} / \left((\eta^{\text{ev}})^2 (\eta^{\text{conv}})^4\right). \tag{47}$$

Clearly, it covers the ideal efficiency scenarios where $\eta^{\text{ev}} = \eta^{\text{conv}} = 1$ (Proposition 2).

Using Eqs 45–47 and based on the theoretical results for the ideal efficiency configuration, here, a procedure is proposed to compute a near-optimal output power $p_{\mathrm{TOU}}^{\mathrm{v2g}}$ for the uniform realistic efficiency scenario. The procedure is as follows:

1. We evaluate the scheduler (9)–(32) at $P^{\mathrm{v2g}} = 0$ and $P^{\mathrm{v2g}} = P_{\mathrm{DN-}}$, obtaining c^{imp} (0), c^{imp} ($P_{\mathrm{DN-}}$), and e^{nff} ($P_{\mathrm{DN-}}$).
2. We compute the V2G output power capacity $p_{\mathrm{cap}}^{\mathrm{v2g}}$ using Eq. 45 with $p = P_{\mathrm{DN-}}$.
3. We compute the near-optimal V2G output power $p_{\mathrm{TOU}}^{\mathrm{v2g}}$ using Eq. 43 with Eqs 46, 47. In Eq. 43, $c^{\mathrm{imp}}\left(p_{\mathrm{cap}}^{\mathrm{v2g}}\right)$ is substituted with c^{imp} ($P_{\mathrm{DN-}}$) since they are equal according to Proposition 1.

The V2G output power $p_{\mathrm{TOU}}^{\mathrm{v2g}}$, previously computed for the uniform realistic efficiency scenario , is said to be near-optimal, in the sense that it is within the vicinity of an optimal point where any V2G output power greater than it does not bring any more profit. This is to be verified in the following evaluation results.

Let the V2G unit sale price $S^{\mathrm{v2g}} = C_2^{\mathrm{TOU}} - 4¢/\mathrm{kWh}$. Figure 10 shows the V2G day profit $\Pr(p)$ profiles with the output time interval $\mathcal{T}^{\mathrm{v2g}} = [13{:}00, 14{:}00]$ for different peak-hour scenarios. The day profit values in Figure 10 were evaluated for a discrete-value set of V2G output power, with a sampling interval of 10 kW. It can be observed that the optimal output power (where the maximum profit is achieved) for Figure 10A is within (160kW, 180 kW), and the optimal output power for Figure 10B is within (60kW, 70 kW). As shown in Figure 10, the suggested computed output power $p_{\mathrm{TOU}}^{\mathrm{v2g}}$ is near the optimal output power in both cases.

Finally, it is also interesting to study the relationship between the possible range of V2G energy sale prices and the output power. Figure 11 shows the average unit cost $C_{\mathrm{a}}^{\mathrm{v2g}}(p)$ profiles as functions of the V2G output power for different scenarios. It should be noted that the V2G sale price must be greater than the average unit cost $C_{\mathrm{a}}^{\mathrm{v2g}}(p)$ and smaller than the peak TOU price C_2^{TOU}. It can be seen that at $p = p_{\mathrm{TOU}}^{\mathrm{v2g}}$, there is much space for choosing the sale price within $\left[C_{\mathrm{a}}^{\mathrm{v2g}}(p), C_2^{\mathrm{TOU}}\right]$. Therefore, in the sense of making a larger range of possible V2G sale prices, $p_{\mathrm{TOU}}^{\mathrm{v2g}}$ is also a good choice for the V2G output power.

7 Conclusion

Many studies in the field of V2G focus on efficient charging strategies and grid stability maintenance. However, a prerequisite for implementing these functionalities lies in accurately predicting the user demands and, consequently, being able to further forecast the capacity of V2G services provided by charge parks. This paper aims to promote the adoption of EV technologies and focuses on the practical operating paradigm of charge park V2G service businesses, with the objective of maximizing profit and enhancing customer interaction. The operating paradigm involves determining a service agreement and conducting two consecutive day-ahead analyses. The design principles of a service agreement are emphasized in the paper, and a practical service agreement is formulated based on these principles. Additionally, a V2G energy reserve modeling method is developed for the rapid estimation of V2G energy reserve distribution in the first day-ahead analysis. This method is applied in a case study of charge parks in the working and recreational environment of New York City. Furthermore, this paper proposes an evaluation framework for the second day-ahead analysis, which offers various metrics to characterize the V2G output capacity. The evaluation metrics and profit maximization methods are presented with theoretical results and are validated through computer experiments. These findings contribute to the understanding and optimization of V2G operations. In conclusion, this paper advocates for the adoption of EV technologies by addressing the practical operating paradigm of charge park V2G service businesses. The study highlights the design principles of a service agreement, develops a V2G energy reserve modeling method, and proposes an evaluation framework for the V2G output capacity. The presented theoretical and experimental results provide valuable insights for maximizing profit and optimizing the utilization of EVs in the V2G context.

Data availability statement

The original contributions presented in the study are included in the article/Supplementary Material, further inquiries can be directed to the corresponding author.

Author contributions

Conceptualization: CP; methodology: CP; software: CP; validation: CP; formal analysis: CP; investigation: YN; data curation: YN; writing—original draft preparation: CP and YN; writing—review and editing: CP; visualization: CP and YN; supervision: CP; project administration: CP; and funding acquisition: CP. All authors contributed to the article and approved the submitted version.

Funding

This work was supported by the Natural Science Foundation of China under Grant 62006095, the Natural Science Foundation of Hunan Province, China, under Grant 2021JJ40441, the Research Foundation of Education Bureau of Hunan Province, China, under Grant 20B470, and the Jishou University Graduate Research and Innovation Project XXJD202204.

Conflict of interest

The authors declare that the research was conducted in the absence of any commercial or financial relationships that could be construed as a potential conflict of interest.

Publisher's note

References

Bayram, I. S., Michailidis, G., Devetsikiotis, M., and Parkhideh, B. (2012). "Strategies for competing energy storage technologies for in DC fast charging stations," in 2012 IEEE 3rd Int. Conf. Smart Grid Commun. (SmartGridComm) (IEEE), 1–6.

Chai, Y. T., Che, H. S., Tan, C., Tan, W.-N., Yip, S.-C., and Gan, M.-T. (2023). A two-stage optimization method for vehicle to grid coordination considering building and electric vehicle user expectations. *Int. J. Electr. Power Energy Syst.* 148, 108984. doi:10.1016/j.ijepes.2023.108984

Dai, S., Gao, F., Guan, X., Yan, C.-B., Liu, K., Dong, J., et al. (2020). Robust energy management for a corporate energy system with shift-working v2g. *IEEE Trans. Autom. Sci. Eng.* 18, 650–667. doi:10.1109/tase.2020.2980356

Fan, P., Sainbayar, B., and Ren, S. (2015). Operation analysis of fast charging stations with energy demand control of electric vehicles. *IEEE Trans. Smart Grid* 6, 1819–1826. doi:10.1109/tsg.2015.2397439

Gough, R., Dickerson, C., Rowley, P., and Walsh, C. (2017). Vehicle-to-grid feasibility: A techno-economic analysis of EV-based energy storage. *Appl. Energy* 192, 12–23. doi:10.1016/j.apenergy.2017.01.102

Hoehne, C. G., and Chester, M. V. (2016). Optimizing plug-in electric vehicle and vehicle-to-grid charge scheduling to minimize carbon emissions. *Energy* 115, 646–657. doi:10.1016/j.energy.2016.09.057

Hu, H., Fang, M., Hu, F., Zeng, S., and Deng, X. (2021). A new design of substation grounding based on electrolytic cathodic protection and on transfer corrosion current. *Electr. Power Syst. Res.* 195, 107174. doi:10.1016/j.epsr.2021.107174

Huang, B., Meijssen, A. G., Annema, J. A., and Lukszo, Z. (2021). Are electric vehicle drivers willing to participate in vehicle-to-grid contracts? A context-dependent stated choice experiment. *Energy Policy* 156, 112410. doi:10.1016/j.enpol.2021.112410

Huda, M., Koji, T., and Aziz, M. (2020). Techno economic analysis of vehicle to grid (v2g) integration as distributed energy resources in Indonesia power system. *Energies* 13, 1162. doi:10.3390/en13051162

Huo, B., Wang, Z., and Tian, Y. (2016). The impact of justice on collaborative and opportunistic behaviors in supply chain relationships. *Int. J. Prod. Econ.* 177, 12–23. doi:10.1016/j.ijpe.2016.04.006

Islam, M. S., Mithulananthan, N., and Lee, K. Y. (2018). Suitability of PV and battery storage in EV charging at business premises. *IEEE Trans. Power Syst.* 33, 4382–4396. doi:10.1109/tpwrs.2017.2774361

Jin, J., and Tan, M. (2019). Low power quadrature voltage controlled oscillator. *Int. J. RF Microw. Computer-Aided Eng.* 29, e21952. doi:10.1002/mmce.21952

Jin, J., and Zhao, L. (2018). Low voltage low power fully integrated chaos generator. *J. Circuits, Syst. Comput.* 27, 1850155. doi:10.1142/s0218126618501554

Lakshminarayanan, V., Chemudupati, V. G. S., Pramanick, S., and Rajashekara, K. (2018). "Real-time optimal energy management controller for electric vehicle integration in workplace microgrid," in IEEE Transactions on Transportation Electrification.

Li, C., Shi, X., Liang, S., Ma, X., Han, M., Wu, X., et al. (2020a). Spatially homogeneous copper foam as surface dendrite-free host for zinc metal anode. *Chem. Eng. J.* 379, 122248. doi:10.1016/j.cej.2019.122248

Li, S., Gu, C., Li, J., Wang, H., and Yang, Q. (2020b). Boosting grid efficiency and resiliency by releasing v2g potentiality through a novel rolling prediction-decision framework and deep-lstm algorithm. *IEEE Syst. J.* 15, 2562–2570. doi:10.1109/jsyst.2020.3001630

Lopez-Behar, D., Tran, M., Froese, T., Mayaud, J. R., Herrera, O. E., and Merida, W. (2019). Charging infrastructure for electric vehicles in multi-unit residential buildings: Mapping feedbacks and policy recommendations. *Energy Policy* 126, 444–451. doi:10.1016/j.enpol.2018.10.030

Maigha, and Crow, M. L. (2017). Cost-constrained dynamic optimal electric vehicle charging. *IEEE Trans. Sustain. Energy* 8, 716–724. doi:10.1109/tste.2016.2615865

Mauri, G., and Valsecchi, A. (2012). "Fast charging stations for electric vehicle: The impact on the MV distribution grids of the Milan metropolitan area," in 2012 IEEE Int. Energy Conf. and Exhibition (ENERGYCON) (IEEE), 1055–1059.

Mouli, G. R. C., Kefayati, M., Baldick, R., and Bauer, P. (2017). Integrated PV charging of EV fleet based on energy prices, V2G and offer of reserves. *IEEE Trans. Smart Grid* 10, 1313–1325. doi:10.1109/TSG.2017.2763683

Nguyen, H. N., Zhang, C., and Zhang, J. (2016). Dynamic demand control of electric vehicles to support power grid with high penetration level of renewable energy. *IEEE Trans. Transp. Electrific.* 2, 66–75. doi:10.1109/tte.2016.2519821

Popkova, E. G., Bogoviz, A. V., and Sergi, B. S. (2023). Editorial: Smart grids and energytech as a way for sustainable and environmental development of energy economy. *Front. Energy Res.* 11, 246. doi:10.3389/fenrg.2023.1145234

Qin, D., Sun, Q., Wang, R., Ma, D., and Liu, M. (2020). Adaptive bidirectional droop control for electric vehicles parking with vehicle-to-grid service in microgrid. *CSEE J. Power Energy Syst.* 6, 793–805. doi:10.17775/CSEEJPES.2020.00310

Rahmani-Andebili, M., and Fotuhi-Firuzabad, M. (2017). An adaptive approach for pevs charging management and reconfiguration of electrical distribution system penetrated by renewables. *IEEE Trans. Indust. Inf.* 14, 2001–2010. doi:10.1109/tii.2017.2761336

Ravi, S. S., and Aziz, M. (2022). Utilization of electric vehicles for vehicle-to-grid services: Progress and perspectives. *Energies* 15, 589. doi:10.3390/en15020589

Richardson, P., Flynn, D., and Keane, A. (2012). Optimal charging of electric vehicles in low-voltage distribution systems. *IEEE Trans. Power Syst.* 27, 268–279. doi:10.1109/tpwrs.2011.2158247

Shan, L., Zhou, J., Zhang, W., Xia, C., Guo, S., Ma, X., et al. (2019). Highly reversible phase transition endows v6o13 with enhanced performance as aqueous zinc-ion battery cathode. *Energy Technol.* 7, 1900022. doi:10.1002/ente.201900022

Shi, S., Wang, Y., and Jin, J. (2023). Multi-agent-based control strategy for centerless energy management in microgrid clusters. *Front. Energy Res.* 11, 239. doi:10.3389/fenrg.2023.1119461

Singh, P. P., Das, S., Wen, F., Palu, I., Singh, A. K., and Thakur, P. (2023). Multi-objective planning of electric vehicles charging in distribution system considering priority-based vehicle-to-grid scheduling. *Swarm Evol. Comput.* 77, 101234. doi:10.1016/j.swevo.2023.101234

Song, D., Yang, Y., Zheng, S., Deng, X., Yang, J., Su, M., et al. (2020). New perspectives on maximum wind energy extraction of variable-speed wind turbines using previewed wind speeds. *Energy Convers. Manag.* 206, 112496. doi:10.1016/j.enconman.2020.112496

Suul, J. A., D'Arco, S., and Guidi, G. (2016). Virtual synchronous machine-based control of a single-phase bi-directional battery charger for providing vehicle-to-grid services. *IEEE Trans. Ind. Appl.* 52, 3234–3244. doi:10.1109/tia.2016.2550588

Szinai, J. K., Sheppard, C. J., Abhyankar, N., and Gopal, A. R. (2020). Reduced grid operating costs and renewable energy curtailment with electric vehicle charge management. *Energy Policy* 136, 111051. doi:10.1016/j.enpol.2019.111051

Triviño-Cabrera, A., Aguado, J. A., and de la Torre, S. (2019). Joint routing and scheduling for electric vehicles in smart grids with v2g. *Energy* 175, 113–122. doi:10.1016/j.energy.2019.02.184

Uddin, K., Jackson, T., Widanage, W. D., Chouchelamane, G., Jennings, P. A., and Marco, J. (2017). On the possibility of extending the lifetime of lithium-ion batteries through optimal v2g facilitated by an integrated vehicle and smart-grid system. *Energy* 133, 710–722. doi:10.1016/j.energy.2017.04.116

Varshosaz, F., Moazzami, M., Fani, B., and Siano, P. (2019). Day-ahead capacity estimation and power management of a charging station based on queuing theory. *IEEE Trans. Indust. Inf.* 15, 5561–5574. doi:10.1109/tii.2019.2906650

Wang, Z., Huo, B., Tian, Y., and Hua, Z. (2015). Effects of external uncertainties and power on opportunism in supply chains: Evidence from China. *Int. J. Prod. Res.* 53, 6294–6307. doi:10.1080/00207543.2015.1053578

Wu, C.-S., Peng, Y.-X., Zhuo, D.-B., Zhang, J.-Q., Ren, W., and Feng, Z.-Y. (2022). Energy ratio variation-based structural damage detection using convolutional neural network. *Appl. Sci.* 12, 10220. doi:10.3390/app122010220

Yan, Q., Zhang, B., and Kezunovic, M. (2018). Optimized operational cost reduction for an EV charging station integrated with battery energy storage and PV generation. *IEEE Trans. Smart Grid* 10, 2096–2106. doi:10.1109/tsg.2017.2788440

Yunus, K., De La Parra, H. Z., and Reza, M. (2011). "Distribution grid impact of plug-in electric vehicles charging at fast charging stations using stochastic charging model," in Proceedings of the 2011 14th European Conference on Power Electronics and Applications (IEEE), 1–11.

Zhang, H., Hu, Z., Xu, Z., and Song, Y. (2016). Evaluation of achievable vehicle-to-grid capacity using aggregate pev model. *IEEE Trans. Power Syst.* 32, 784–794. doi:10.1109/tpwrs.2016.2561296

Zhang, H., Li, P., Jin, H., Bi, R., and Xu, D. (2022). Nonlinear wave energy dissipator with wave attenuation and energy harvesting at low frequencies. *Ocean. Eng.* 266, 112935. doi:10.1016/j.oceaneng.2022.112935

Zhao, H., Zhang, H., Bi, R., Xi, R., Xu, D., Shi, Q., et al. (2020). Enhancing efficiency of a point absorber bistable wave energy converter under low wave excitations. *Energy* 212, 118671. doi:10.1016/j.energy.2020.118671

Zhu, L., Hu, R., Xiang, Y., Yang, X., Chen, Z., Xiong, L., et al. (2021). Enhanced performance of li-s battery by constructing inner conductive network and outer adsorption layer sulfur-carbon composite. *Int. J. Energy Res.* 45, 6002–6014. doi:10.1002/er.6220

Nomenclature

Q14

Acronyms	
AIP	Average import price
BC	Business charging
CC	Commercial charging
CDnf	Charge-demand-not-fulfilled
Ecost	Imported electricity cost
ESS	Electricity storage system
EV	Electric vehicle
FCS	Fast charging station
HC	Home charging
MP	Marginal profit
NHTS	National Household Travel Survey
SoC	State-of-charge
TOU	Time-of-use
V2G	Vehicle-to-grid
VMT	Vehicle Miles of Travel
NYISO	New York Independent System Operator
Symbols- V2G energy reserve estimation	
$[l(\cdot)]$	Length of a Lebesgue-measurable subset of the set of real numbers $\mathbb{R}$
$[p_c]$	Rated charge power for an EV (kW)
$[p_{ca}]$	Committed average charge power for each EV (kW) according to the service agreement
$[p_d]$	Rated discharge power for an EV (kW)
$[s_0]$	Initial SoC of an EV at arrival
$[T_1]$	Maximum discharge period for a modeled EV (h)
$[T_2]$	Maximum charge period for a modeled EV in the maximal discharge case (h)
$[t_0]$	Arrival time of an EV
$[t_f]$	Departure time of an EV
$[r(t)]$	V2G energy reserve of an EV at time t (kWh)
$[E^{target}]$	Charge demand of an EV (kWh)
$[s^{max}]$	Maximum SoC for an EV battery to reach by charging
$[s^{target}]$	Planned departure SoC of an EV as a result of its charge demand
Symbols- V2G scheduler model	
Optimization input parameters	
$[B_v^a]$	Battery energy of EV v upon arrival (kWh)
$[\eta_v^+]$	Efficiency of charging the battery of EV v
$[\eta_v^-]$	Efficiency of discharging the battery of EV v
$[B_v^{min}]$	Minimum battery energy of EV v reachable through charge scheduling (kWh)
$[B_v^{max}]$	Maximum battery energy of EV v reachable through charge scheduling (kWh)
$[C^p]$	Penalty for failing to satisfy the charge demand (¢/kWh)
$[\Delta T]$	Time step length for the scheduler (h)
$[C_t^{buy}]$	Grid electricity import price at time t (¢/kWh)

$[N_c^{\mathrm{ch}}]$	Maximum number of EVs that can be simultaneously charged from cth EV–PV converter
$[\eta_c^{\mathrm{conv}}]$	Rated efficiency of charging station c
$[P_c^{\mathrm{EVr}}]$	Rated power capacity of each EV charger in multiplexed charging station c (kW)
$[P^{\mathrm{v2g}}]$	Committed constant V2G output power of the charge park during the output period (kW)
$[T^{\mathrm{v2g}}]$	V2G output period
$[P_t^{\mathrm{DN+}}]$	Distribution network limits for drawing power from the grid (kW)
$[P_t^{\mathrm{DN-}}]$	Distribution network limits for feeding power to the grid (kW)
$[P_c^{\mathrm{conv}}]$	Rated power capacity of the DC/AC inverter of the multiplexed charging station c (kW)
$[K_{v,t,c}]$	Binary variable indicating the connection status of EV v with charging station c at time t
$[N_c^{\mathrm{conn}}]$	Maximum number of EVs that can be connected to the multiplexed charging station c
$[E_v^{\mathrm{target}}]$	Charge demand of EV v (kWh)
Optimization variables	
$[a_{c,t}^{\mathrm{feed}}]$	Binary variable indicating whether charging station c is feeding (1) power to or drawing (0) power from the grid
$[a_{v,t}^{\mathrm{act}}]$	Binary variable indicating whether EV v is active (charging/discharging) or idle at time t
$[a_{v,t}^{\mathrm{v2g}}]$	Binary variable indicating whether EV v is discharging (1) or charging (0)
$[a_t^{\mathrm{exp}}]$	Binary variable indicating whether the charge park is exporting (1) power to or importing power (0) from the grid
$[b_{v,t}]$	Battery energy of EV v at time t (kWh)
$[p_t^{\mathrm{imp}}]$	Power imported from the grid by the charge park at time t (kWh)
$[p_t^{\mathrm{exp}}]$	Power exported to the grid by the charge park at time t (kWh)
$[p_{c,t}^{\mathrm{draw}}]$	Power drawn to the charge park by the charging station c at time t (kW)
$[p_{c,t}^{\mathrm{feed}}]$	Power fed to the charge park by the charging station c at time t (kW)
$[x_{v,t}^{\mathrm{e+}}]$	Charging power of EV v at time t (kW)
$[x_{v,t}^{\mathrm{e-}}]$	Discharging power of EV v at time t (kW)
Symbols- evaluation of V2G service capability	
$[\eta^{\mathrm{ev}}]$	Battery efficiency parameter under the uniform efficiency assumption
$[t_1^{\mathrm{peak}}]$	Start time of the on-peak period
$[t_2^{\mathrm{peak}}]$	End time of the on-peak period
$[C_1^{\mathrm{buy}}]$	Off-peak electricity price in the two-price TOU pricing plan (¢/kWh)
$[C_2^{\mathrm{buy}}]$	On peak electricity price in the two-price TOU pricing plan (¢/kWh)
$[\mathbf{Pr}(\boldsymbol{p})]$	Profit of the V2G service (¢)
$[p_{\mathrm{max}}^{\mathrm{v2g}}]$	Maximum possible V2G output power, when neglecting distribution network constraints
$[p_{\mathrm{TOU}}^{\mathrm{v2g}}]$	V2G output power threshold (kW)
$[p^{\mathrm{v2g}}]$	V2G output power capacity, i.e., maximum output power p such that CDnf can be kept as zero
$[S^{\mathrm{v2g}}]$	V2G energy sell price (¢/kWh)
$[\mathbf{MP}(\boldsymbol{p})]$	V2G service marginal profit (¢/kWh)
$[T_{\mathrm{peak}}^{\mathrm{TOU}}]$	On-peak period in the TOU pricing plan
$[T_{\mathrm{off-peak}}^{\mathrm{TOU}}]$	Off-peak period in the TOU pricing plan
$[C_{\delta p}^{\mathrm{v2g}}(\boldsymbol{p})]$	V2G energy incremental unit cost (¢/kWh)
$[C^{\mathrm{v2g}}(\boldsymbol{p})]$	V2G energy marginal cost (¢/kWh)
$[C_{\mathrm{a}}^{\mathrm{v2g}}(\boldsymbol{p})]$	V2G energy average unit cost (¢/kWh)
C_1^{v2g}, C_2^{v2g}	Characteristic marginal costs of the V2G service under a two-price TOU plan (¢/kWh)
e^{nff}, $e^{\mathrm{nff}}(\boldsymbol{p})$	Charge-demand-not-fulfilled (kWh)
c^{imp}, $c^{\mathrm{imp}}(\boldsymbol{p})$	Total imported electricity cost (¢)